International Journal of Design & Nature and Ecodynamics
Vol. 21, No. 8, August, 2026, pp. 2259-2273
Journal homepage: http://iieta.org/journals/ijdne

GIS-Based Evaluation of Land Use Structure and Agricultural Potential in the Newly Delimited Almaty Region, Kazakhstan

Yerzhan Zhussupov, Aizhan Zhildikbayeva*, Timur Rafikov

Department of Land Resources and Cadastre, Kazakh National Agrarian Research University, Almaty 050010, Kazakhstan

Corresponding Author Email: a.zhildikbayeva@mymail.academy

https://doi.org/10.18280/ijdne.210808

Received: 27 January 2026
Revised: 12 August 2026
Accepted: 20 August 2026
Available online: 31 August 2026

Keywords:
administrative boundary change, agricultural land suitability, GIS-based multi-criteria evaluation, land-cover change detection, NDVI time series, spatial prioritization, optimization model, land use planning

ABSTRACT

Administrative boundary reform can produce apparent changes in land statistics when reporting units are redefined. This study separately analyzed official legal land categories, satellite-derived physical land cover, Normalized Difference Vegetation Index (NDVI), and scenario-based agricultural suitability in the newly delimited Almaty Region, Kazakhstan. Official land-balance records for 2019–2023 were combined with Sentinel-2 growing-season NDVI composites, 2021 and 2023 Esri/Impact Observatory land-cover maps, the Copernicus Digital Elevation Model, OpenStreetMap data, and constrained multi-criteria modeling. The 53.0% reduction in the reported regional area in 2022 reflected the creation of the Zhetysu Region rather than physical land loss. Between 2022 and 2023, official agricultural land increased by 216.0 thousand ha and reserve land decreased by 212.8 thousand ha. These changes were not matched to individual parcels and are not directly comparable with the approximately 137 thousand ha net cropland gain detected by the separate 2021–2023 satellite analysis because the datasets represent different objects, periods, and spatial coverage. Mean and median growing-season NDVI were lower in 2023 than in 2019, but no attribution to climate variability or land-use change was attempted. The conservation-oriented scenario was the most spatially stable, and approximately 312.6 thousand ha were included in the priority set under all three scenarios. These zones represent screening priorities rather than verified reserve land and should be validated through cadastral checks and soil, water, and field assessments before being used to inform planning decisions.

1. INTRODUCTION

The rational and sustainable use of land resources is essential for food security [1, 2], climate resilience, ecosystem conservation, and balanced regional development [3]. Agricultural territories are increasingly affected by land degradation, spatial fragmentation, urban expansion, and competition among productive, residential, infrastructural, and environmental functions [4, 5]. When land management is based predominantly on aggregated statistical inventories, it may indicate changes in the total area of land categories but does not reveal where those changes occurred [6], which land-cover classes were transformed, or whether the observed differences resulted from physical land conversion or from the redelimitation of administrative boundaries [7-9].

The Almaty Region represents a particularly important case because it combines irrigated and rainfed agriculture, foothill and mountain landscapes, major transport corridors, protected natural areas, and strong market pressure associated with the Almaty metropolitan area [10]. The south-eastern agricultural zone of Kazakhstan, which includes the Almaty and Zhambyl Regions, contains more than 1.7 million ha of field crops [11]. The estimated share of irrigated land is approximately 46% in the Almaty Region and 65% in the Zhetysu Region. Agricultural production in this zone includes winter wheat, spring barley, maize, soybean, safflower, potatoes, vegetables, and fruit crops. This production diversity means that the suitability and intensity of agricultural land use depend not only on vegetation condition but also on water availability, terrain, transport accessibility, proximity to markets, and environmental restrictions [12]. Research conducted in the Karasai District has additionally demonstrated that intensive agricultural use is accompanied by land-degradation risks and requires integrated information monitoring and ecosystem-based management [13].

The administrative reorganization of 2022 introduced an additional spatial and methodological challenge. Under Presidential Decree No. 887, the Zhetysu Region was formed by separating eight districts and the cities of Taldykorgan and Tekeli from the former Almaty Region, while the administrative centre of the newly delimited Almaty Region was transferred to Konaev [14]. The decree entered into force on 8 June 2022. Consequently, the statistical territory referred to as the “Almaty Region” after 2022 is substantially different from the territory represented by the same name in the 2019–2021 records. A direct comparison of regional totals across this boundary change may therefore confuse administrative redistribution with actual transformation of land use.

This distinction is particularly important because official land-fund categories and remotely sensed land-cover classes represent different characteristics of the territory. Official statistics describe the legal and administrative allocation of land to agricultural, settlement, industrial, protected, forest, water, and reserve categories. Satellite observations, by contrast, identify physical surface characteristics such as cropland, grassland, shrub cover, tree cover, built-up areas, bare ground, and water [15]. A decrease in the official area of reserve land accompanied by an increase in agricultural land cannot by itself prove that the same parcels physically changed from one land-cover class to another. Reliable assessment therefore requires the parallel, but methodologically separate, analysis of legal land-category statistics and satellite-derived land-cover transitions.

Remote sensing and GIS make it possible to analyze administrative records and physical land-cover change in parallel while preserving the different meanings, spatial units, and classification systems of the two evidence streams [16, 17]. The Esri/Impact Observatory annual 10-m land-use/land-cover series supports post-classification comparison, while Sentinel-2 enables annual Normalized Difference Vegetation Index (NDVI) assessment [18-21]. Previous research in the Almaty Region examined NDVI for 2015, 2020, and 2023 [22] and described land-use dynamics and crop distribution during 2019–2023 [23], but did not combine boundary overlay, class-to-class transition analysis, and explicit suitability modeling.

GIS-based multi-criteria evaluation can integrate vegetation, terrain, infrastructure accessibility, and environmental constraints, provided that the objectives, variables, weights, exclusion rules, scenarios, and sensitivity procedures are clearly defined [24-30]. The remaining research gap is therefore the absence of an integrated framework that harmonizes administrative boundaries, analyzes official land-category statistics and satellite-derived land-cover transitions separately, and interprets them as complementary but non-equivalent evidence within the post-reform territory.

This study developed such a framework for the newly delimited Almaty Region. It aimed to: (i) quantify official land-fund dynamics during 2019–2023; (ii) compare land structures on both sides of the new administrative boundary; (iii) assess annual NDVI trajectories and 2021–2023 land-cover transitions; and (iv) compare balanced, conservation-oriented, and production-accessibility scenarios. Official land categories and satellite-derived land cover were analyzed separately and treated as complementary but non-equivalent evidence; no one-to-one correspondence between legal category changes and physical land-cover transitions was assumed.

2. MATERIALS AND METHODS

2.1 Study area and temporal design

The study area comprises the newly delimited Almaty Region in south-eastern Kazakhstan and covers approximately 105,089 km² according to the 2023 official land balance. It includes irrigated and rainfed agricultural areas, foothill and mountain landscapes, protected territories, and rapidly expanding peri-urban areas surrounding the Almaty metropolitan area. Under Presidential Decree No. 887 of 3 May 2022, effective from 8 June 2022, the Zhetysu Region was created from part of the former Almaty Region, and the administrative centre of the newly delimited Almaty Region was transferred from Taldykorgan to Konaev [14]. The former regional boundary was reconstructed as the union of the present-day Almaty and Zhetysu Regions (Figure 1).

The years 2019–2021 were treated as the pre-division period, 2022 as the reform year, and 2023 as the first post-division year. Changes between 2021 and 2022 were interpreted primarily as the statistical effect of boundary redefinition, whereas changes between 2022 and 2023 were assessed within the newly delimited Almaty Region. Physical land-cover changes were evaluated separately for 2021–2023.

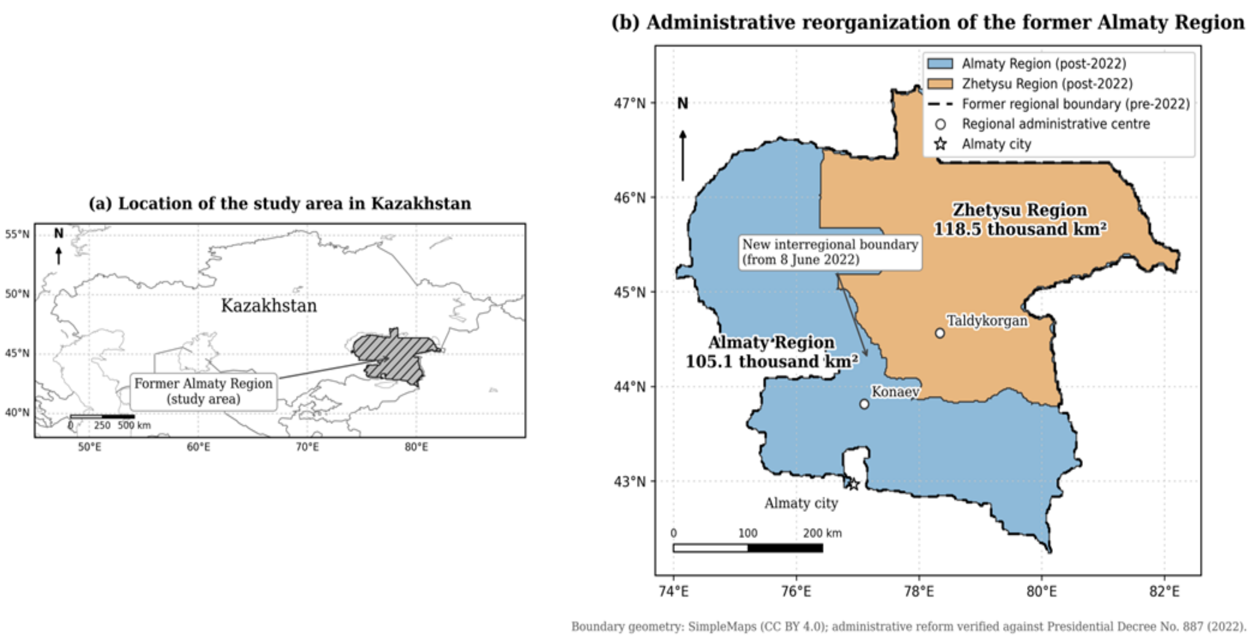

Figure 1. Study area and administrative reorganization of the former Almaty Region: (a) location of the former Almaty Region within Kazakhstan, and (b) post-2022 boundaries of the Almaty and Zhetysu Regions, with the former regional boundary shown for comparison

Note: The former Almaty Region was reconstructed as the union of the present-day Almaty and Zhetysu Regions. Boundary geometry was obtained from SimpleMaps under the CC BY 4.0 license and verified against Presidential Decree No. 887 of 3 May 2022 [14, 31].

2.2 Data sources

Official land-balance statistics for 2019–2023 were obtained from the Committee for Land Resource Management and regional statistical records [32]. Administrative boundaries were obtained from the SimpleMaps Kazakhstan dataset and verified against Presidential Decree No. 887 [14, 31].

Annual vegetation conditions were derived from harmonized Sentinel-2 Level-2A surface-reflectance data at 10-m resolution [33, 34]. Physical land-cover transitions were assessed using the 2021 and 2023 Esri/Impact Observatory annual land-use/land-cover maps, also provided at 10-m resolution [21]. Terrain slope was calculated from Copernicus DEM GLO-30 [35], while roads, settlements, rivers, reservoirs, and mapped irrigation features were obtained from OpenStreetMap [36]. Specially protected natural areas were derived from the protected-area polygons available in OpenStreetMap [36].

Spatial processing was performed in QGIS 3.22, ArcGIS 10.8, Google Earth Engine, and Python 3.11. Because complete parcel-level cadastral polygons were unavailable, official land-balance data were used to represent legal categories and satellite products to represent physical land cover; these datasets were analyzed separately.

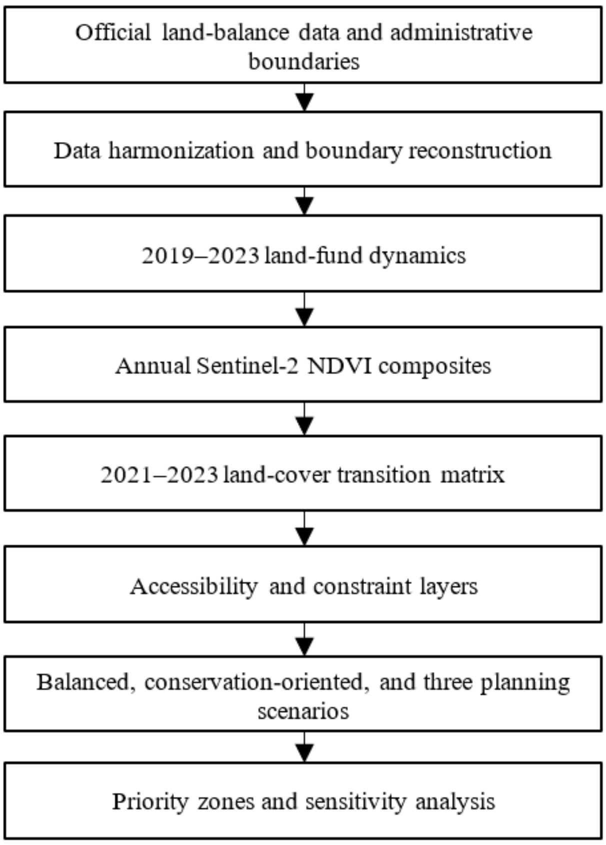

Figure 2. Workflow for land-fund analysis, Normalized Difference Vegetation Index (NDVI) processing, land-cover change detection, suitability modeling, and sensitivity assessment

Official land statistics and satellite land-cover data were used to address different questions: the former describe legal and administrative land categories, whereas the latter describe physical surface cover. The study did not attempt a one-to-one match between legal category changes and parcel-level physical transitions because a complete georeferenced cadastral parcel layer was unavailable. The two data streams were therefore analyzed separately and interpreted as complementary but non-equivalent evidence. In particular, the 2022–2023 official changes within the newly delimited Almaty Region were not treated as quantitatively equivalent to the 2021–2023 satellite-derived changes calculated for the former regional territory.

The analytical workflow is summarized in Figure 2.

2.3 Spatial preprocessing and boundary harmonization

All vector datasets were initially stored in the WGS 84 geographic coordinate system. Topological checks were performed to identify invalid geometries, self-intersections, duplicate polygons, gaps, and overlaps. The pre-reform boundary was reconstructed by merging the post-reform Almaty and Zhetysu regional polygons. The resulting area was compared with the combined official area of the two successor regions, and a maximum discrepancy of 1% was adopted as the quality-control tolerance. Official land-balance totals remained authoritative when minor differences arose between vector-derived and reported areas.

Area calculations and raster cross-tabulation were conducted in the WGS 84/NSIDC EASE-Grid 2.0 Global equal-area coordinate system (EPSG:6933). Distance and buffer operations were performed separately in WGS 84/UTM Zone 43N and WGS 84/UTM Zone 44N because the study territory crosses both zones. The results were subsequently mosaicked into a common regional layer.

All raster datasets were aligned to a common 100 × 100 m analytical grid in EPSG:6933. Each grid cell therefore represented 1 ha. The 100-m decision unit was selected to reduce isolated classification noise and computational demand while retaining sufficient spatial detail for regional land-use planning. Categorical rasters were aggregated using the majority class, whereas continuous variables, including NDVI, elevation, slope, and distance surfaces, were resampled using bilinear interpolation.

2.4 Official land-fund dynamics and administrative-boundary comparison

Annual changes in the official land-fund categories were calculated in both absolute and relative terms:

$$\Delta A_{c,t} = A_{c,t} - A_{c,t-1} \quad (1)$$

$$R_{c,t} = \frac{A_{c,t} - A_{c,t-1}}{A_{c,t-1}} \times 100 \quad (2)$$

where, $A_{c,t}$ is the area of land category c in year t, $A_{c,t-1}$ is the area of the same land category in the previous year, $\Delta A_{c,t}$ is the annual absolute change, and $R_{c,t}$ is the annual percentage change.

The 2019–2021 values were used to characterize the land-fund structure of the former Almaty Region. The 2022 values were used to compare the two successor regions immediately after the administrative division, and the 2022–2023 comparison was used to assess changes occurring within the newly delimited Almaty Region.

To determine differences on both sides of the new boundary, the proportional structure of each legal land category was calculated separately for the Almaty and Zhetysu Regions:

$$P_{r,c} = \frac{A_{r,c}}{\sum_{c=1}^{n} A_{r,c}} \times 100 \qquad (3)$$

where, $P_{r,c}$ is the percentage share of category c in region r, and $A_{r,c}$ is its area. Absolute areas and percentage shares were compared for agricultural, settlement, industrial and transport, protected, forest, water, and reserve land.

Changes in aggregate legal categories were not interpreted as parcel-level transfers or physical land-cover transitions. No parcel-level correspondence between official category changes and satellite-derived transitions was tested because the required georeferenced cadastral data were unavailable.

2.5 Annual Sentinel-2 Normalized Difference Vegetation Index time-series analysis

Sentinel-2 Level-2A observations acquired during the common growing-season window from 1 May to 30 September were processed separately for each year from 2019 to 2023. Scenes with a metadata cloud-cover value greater than 20% were excluded. Cloud-contaminated and unreliable pixels were masked using the Scene Classification Layer. The excluded classes comprised no-data pixels, saturated or defective pixels, dark features, cloud shadows, unclassified pixels, medium- and high-probability clouds, cirrus clouds, and snow or ice.

NDVI was calculated for each valid observation as:

$$NDVI = \frac{B8 - B4}{B8 + B4} \qquad (4)$$

where, $B8$ is near-infrared surface reflectance, and $B4$ is red surface reflectance. A pixel-wise median composite was then produced for each growing season. Median compositing reduced the influence of residual clouds, atmospheric variation, and anomalous individual observations.

For consistency with the authors' previous regional study, annual NDVI values were grouped into three principal vegetation classes [22]:

•NDVI < 0.20: little or no active vegetation, including open soil, rocks, built-up surfaces, or severely depleted vegetation;

•0.20 ≤ NDVI ≤ 0.40: sparse or moderately developed vegetation;

•NDVI > 0.40: dense and actively developed vegetation.

The thresholds describe vegetation density and should not be interpreted independently as evidence of land degradation or agricultural suitability. For example, a low NDVI value may reflect fallow land, a recently harvested field, exposed soil, or a built-up surface rather than degradation alone. The same thresholds were used primarily to preserve comparability with the authors' earlier NDVI analysis. The earlier publication used B8 and B4 and classified values above 0.4, between 0.2 and 0.4, and below 0.2 in the same manner.

Inter-annual NDVI trajectories were evaluated for pixels containing at least three valid annual observations. A linear trend coefficient was calculated as:

$$\beta_i = \frac{\sum_{t=1}^{5}(t-\bar{t})\left(NDVI_{i,t} - \overline{NDVI}_i\right)}{\sum_{t=1}^{5}(t-\bar{t})^2} \qquad (5)$$

where, β_i is the annual NDVI trend for pixel i. To avoid interpreting very small variations as meaningful change, trajectories were classified as increasing when $\beta_i \geq 0.01$ NDVI units per year, decreasing when $\beta_i \leq -0.01$, and stable when $|\beta_i| < 0.01$. The threshold of 0.01 was adopted as a practical screening rule rather than a universal ecological threshold. Because the series contained only five annual observations, the regression slope was interpreted descriptively and was not used as a formal test of long-term climatic trends.

Precipitation and other climatic or land-management variables were not included in the analysis. Therefore, the observed NDVI trajectories were interpreted descriptively and could not be attributed to either land-use change or climate variability.

Annual mean and median NDVI values and the areas of the three NDVI classes were summarized for the entire study area and, where boundary data permitted, by administrative district.

2.6 Land-cover change detection

Land-cover change was evaluated through post-classification comparison of the 2021 and 2023 Esri/Impact Observatory annual LULC maps. The original classes were aggregated into six analytical groups:

1. cropland;
2. grass and shrub cover, represented by the rangeland class;
3. tree cover;
4. built-up land;
5. bare ground;
6. water and wetland.

Snow, ice, clouds, and no-data pixels were excluded. The 10-m classifications were aggregated to the common 100-m analytical grid using majority assignment. Both annual maps were aligned to an identical spatial extent, cell size, origin, and coordinate system before comparison.

A transition matrix was constructed by cross-tabulating the 2021 and 2023 class values:

$$T_{ij} = \frac{n_{ij} \times a}{10^7} \qquad (6)$$

where, T_{ij} is the area of transition from class i in 2021 to class j in 2023, expressed in thousand ha; n_{ij} is the number of grid cells with the corresponding transition; and a is the area of one grid cell in m². For the 100-m grid, a = 10,000 m², equivalent to 1 ha.

The transition matrix distinguished stable classes on its main diagonal and conversions between classes outside the diagonal. Particular attention was given to:

•rangeland → cropland;

•bare ground → cropland;

•cropland → built-up land;

•cropland → rangeland;

•stable cropland;

•stable tree cover.

The transition analysis was first performed for the complete territory of the former Almaty Region and was then summarized separately within the current Almaty and Zhetysu boundaries. This made it possible to determine both where physical land-cover change occurred and how its spatial pattern differed on the two sides of the new administrative boundary.

Satellite-derived transitions represent changes in physical surface cover and do not establish legal transfer between cadastral categories. Thus, a rangeland-to-cropland transition is not automatically equivalent to a legal reserve-land-to-agricultural-land reclassification.

2.7 Accessibility indicators and spatial constraints

Five continuous suitability and accessibility indicators and one categorical land-cover indicator were prepared:

1. Growing-season median NDVI;
2. Terrain slope derived from Copernicus DEM GLO-30;
3. Euclidean distance to major roads;
4. Euclidean distance to rivers, reservoirs, and mapped irrigation canals;
5. Euclidean distance to settlements and major urban markets;
6. Current land-cover class.

Road analysis included motorway, trunk, primary, secondary, and tertiary road classes. Water-accessibility analysis included rivers, reservoirs, and mapped irrigation canals. Settlement accessibility represented proximity to district centres, Konaev, and the Almaty urban market. OpenStreetMap completeness varies spatially; therefore, these indicators were treated as regional screening variables rather than complete inventories of transport or irrigation infrastructure.

Each criterion was standardized on a common suitability scale from 1 to 9, where 1 represented the least favorable and 9 the most favorable condition.

Table 1. Standardization rules for the agricultural-suitability criteria

Criterion	Score 9	Score 7	Score 5	Score 3	Score 1 or Restriction
Median growing-season Normalized Difference Vegetation Index (NDVI)	>0.40	0.30–0.40	0.20–0.30	0.10–0.20	<0.10
Slope, degrees	0–3	>3–5	>5–8	>8–15	>15: excluded
Distance to a major road, km	≤1	>1–3	>3–5	>5–10	>10
Distance to mapped water or irrigation features, km	≤1	>1–3	>3–5	>5–10	>10
Distance to a settlement or urban market, km	0.5–10	>10–20	>20–40	>40–60	>60; <0.5: excluded
Current land cover	Cropland: 9	-	Rangeland: 6	Bare ground: 4	Trees, built-up land, water/wetland, snow/ice, and no-data: excluded

Note: The class thresholds and distance breakpoints are author-defined regional screening assumptions informed by general land-evaluation principles.

The exclusion mask combined land-cover incompatibilities with conservative, author-defined screening thresholds. Water and wetland, built-up land, tree cover, specially protected natural areas, and cells lacking reliable data were excluded because they were incompatible with the regional agricultural-screening objective or could not be evaluated reliably. The slope threshold of >15° was adopted as a conservative regional assumption reflecting increasing erosion risk and constraints on mechanized cultivation; it was not treated as a statutory threshold [8]. The 100-m buffer around permanent rivers, lakes, and reservoirs corresponded to one analytical grid cell and was used as a precautionary screening margin rather than as a legally delineated water-protection strip. Kazakhstan rules applicable during the study period specified a minimum water-protection-strip width of 35 m, whereas FAO guidance recommends riparian buffers of at least 30 m and wider buffers where slopes are steep, or water bodies adjoin agricultural land [37]. Site-specific legally approved water-protection boundaries must therefore supersede the modeled buffer before implementation.

Hard spatial constraints were represented by a binary exclusion mask. The excluded territories comprised existing water and wetland cells, tree-covered areas, built-up land, specially protected natural areas represented in the available boundary layers, slopes exceeding 15°, and a 100-m protective buffer around permanent rivers, lakes, and reservoirs. Irrigation canals were treated as accessibility features rather than as exclusion zones.

The scores and thresholds in Table 1 were adopted as transparent regional screening assumptions. They are not statutory land-allocation standards and do not replace soil surveys, water-right verification, cadastral examination, or field assessment.

2.8 GIS-based multi-criteria suitability and scenario prioritization

The spatial model was formulated as a constrained multi-criteria prioritization problem. The objective was to identify spatial units with favorable vegetation, terrain, water accessibility, transport accessibility, market accessibility, and land-cover characteristics while excluding environmentally or functionally unsuitable territory.

The final suitability score for spatial unit i was calculated as:

$$S_i = E_i \sum_{j=1}^{m} w_j r_{ij} \tag{7}$$

where, S_i is the composite suitability score, E_i is the binary exclusion mask taking a value of 1 for eligible cells and 0 for excluded cells, r_{ij} is the standardized score of criterion j, and w_j is its relative weight. Criterion weights sum to 1.00, or 100%, when entered into the ArcGIS Weighted Overlay tool. Weighted Overlay requires a common evaluation scale and relative weights summing to 100%.

$$x_i \begin{cases} 1, if\ cell\ i\ is\ selected\ as\ a\ priority\ area \\ 0, otherwise \end{cases} \tag{8}$$

The decision objective was:

$$max\, Z = \sum_{i=1}^{n} S_i x_i \tag{9}$$

subject to:

$$x_i \leq E_i \tag{10}$$

$$\sum_{i=1}^{n} a_i x_i \leq 0.10 \sum_{i=1}^{n} a_i E_i \tag{11}$$

$$x_i \in \{0,1\} \tag{12}$$

where, a_i is the area of cell i. The second constraint limited the high-priority selection to the top 10% of eligible land. This quota was introduced as a common screening condition so that the spatial outputs of alternative scenarios could be directly compared. It does not represent a government target for agricultural expansion.

Cells were ranked from highest to lowest S_i, selected until the 10% area limit was reached, and grouped into contiguous spatial clusters. Isolated clusters smaller than 25 ha were removed because they were considered insufficiently coherent for regional-scale planning.

Three alternative scenarios were modeled. The criterion weights assigned to each scenario are presented in Table 2.

Table 2. Criterion weights used in the land-use scenarios, %

Criterion	Balanced Scenario	Conservation-Oriented Scenario	Production-Accessibility Scenario
Growing-season NDVI	25	15	30
Terrain slope	20	25	10
Proximity to water and irrigation features	20	20	25
Proximity to roads	15	10	20
Proximity to settlements and markets	10	10	10
Current land cover	10	20	5
Total	100	100	100

The numerical weights were assigned by the authors to operationalize three contrasting planning perspectives. They were not derived through formal expert elicitation, stakeholder consultation, AHP, Delphi procedures, or empirical calibration and should therefore be interpreted as study assumptions rather than validated stakeholder preferences. The sensitivity analysis evaluates robustness to moderate weight changes but does not constitute validation of the weighting scheme.

The balanced scenario assigned relatively even importance to productive, environmental, and accessibility factors. The conservation-oriented scenario increased the influence of slope and current land cover to reduce pressure on environmentally sensitive territories. The production-accessibility scenario increased the weights of NDVI, water access, and transport access to identify areas with comparatively favourable production and logistical conditions.

Composite scores were divided into four classes:

- $S_i < 3.0$: low suitability;
- $3.0 \leq S_i < 5.0$: moderately low suitability;
- $5.0 \leq S_i < 7.0$: moderate suitability;
- $S_i \geq 7.0$: high suitability.

The model was designed for regional screening rather than cadastral land allocation. In the absence of complete parcel-level reserve-land polygons, selected cells were interpreted as areas requiring subsequent cadastral verification, soil and water assessment, and field inspection. The total 2.14 million ha of officially reported reserve land was therefore not automatically classified as suitable for agricultural conversion. A spatial overlap analysis between officially designated reserve land and the modeled high-suitability and priority areas was not performed because a complete georeferenced reserve-land layer was unavailable.

2.9 Sensitivity analysis and quality control

The sensitivity of the model was evaluated by varying each criterion weight by ±10% relative to its scenario value and proportionally renormalizing the remaining weights to maintain a total of 100%. The stability of the high-priority zones was evaluated using the Jaccard similarity coefficient:

$$J = \frac{|P_0 \cap P_k|}{|P_0 \cup P_k|} \tag{13}$$

where, P_0 is the set of high-priority cells in the original scenario, and P_k is the corresponding set after weight modification. A value of $J \geq 0.80$ was interpreted as high spatial stability, 0.60–0.79 as moderate stability, and $J < 0.60$ as sensitivity to the weighting assumptions.

Quality-control procedures included verification of raster alignment, comparison of raster-derived and official regional areas, exclusion of cells lacking valid observations in either comparison year, and separate reporting of no-data coverage. All change-detection areas were calculated only for cells with valid land-cover values in both 2021 and 2023.

The principal methodological limitations were the absence of complete parcel-level cadastral polygons, detailed regional soil maps at a scale suitable for parcel-level recommendations, and field validation of all remotely sensed transitions. Accordingly, the model outputs were interpreted as relative spatial priorities rather than definitive evidence of legal land reclassification or immediate agricultural suitability.

3. RESULTS AND DISCUSSION

3.1 Dynamics of the official land fund during 2019–2023

The official land-balance series revealed three analytically distinct stages: the pre-division development of the former Almaty Region during 2019–2021, the immediate statistical effect of administrative re-delimitation in 2022, and the first changes within the newly delimited Almaty Region in 2023. Table 3 presents the areas of the principal legal land categories during the unified analytical period.

During the pre-division period, the total area of the former Almaty Region remained constant at 22,357.2 thousand ha, while the internal distribution of legal land categories changed. Between 2019 and 2021, agricultural land increased by 616.4 thousand ha, or 7.70%, whereas reserve land decreased by 671.3 thousand ha, or 8.56%. Forest fund land increased by 54.8 thousand ha, or 1.48%. Settlement, protected, industrial, and water fund land remained comparatively stable.

The opposite directions of change in agricultural and reserve land are consistent with redistribution within the official land balance. Nevertheless, aggregated annual totals cannot identify whether the same individual parcels were transferred from one legal category to another. They also provide no information about changes in the physical surface cover of those parcels.

The change between 2021 and 2022 was fundamentally different. The area statistically attributed to the Almaty Region decreased by 11,848.2 thousand ha, or approximately 53.0%. This value corresponds to the territory assigned to the newly established Zhetysu Region. The reduction therefore resulted from administrative redelimitation rather than the physical loss, abandonment, or conversion of more than half of the regional territory. The official 2022 land balance reports total areas of 10509.0 thousand ha for the Almaty Region and 11848.2 thousand ha for the Zhetysu Region.

Table 3. Dynamics of the official land-fund structure in the Almaty Region, 2019–2023, thousand ha [32]

Year	Agricultural Lands	Settlement Land	Industrial, Transport, Communications, and Other Non-Agricultural Land	Specially Protected Natural Areas	Forest Fund Land	Water Fund Land	Reserve Land	Total
2019	8007.4	722.6	252.2	1642.7	3695.8	192.0	7844.5	22357.2
2020	8332.5	722.6	257.1	1642.7	3752.2	192.1	7458.0	22357.2
2021	8623.8	723.0	251.8	1642.7	3750.6	192.1	7173.2	22357.2
2022	4310.7	291.7	151.0	962.3	2253.0	187.5	2352.8	10509.0
2023	4526.7	291.7	147.7	962.3	2253.0	187.5	2140.0	10508.9

Note: Percentage changes reported below were calculated by the authors from the official annual land-balance records.

Within the newly delimited Almaty Region, the total land area remained virtually unchanged between 2022 and 2023. Agricultural land increased by 216.0 thousand ha, or 5.01%, while reserve land decreased by 212.8 thousand ha, or 9.04%. Industrial and other non-agricultural land decreased by 3.3 thousand ha, or 2.19%. The combined balance of these changes, +216.0−212.8−3.3= -0.1 thousand ha, corresponds to the minor reduction in the regional total caused by rounding and balance adjustments.

The 216.0 thousand ha increase in official agricultural land should not be compared directly with the approximately 137 thousand ha net increase in the satellite-derived cropland class identified through the separate land-cover transition analysis. The two values refer to different objects – legal land category versus physical land cover – different classification systems, different time intervals (2022–2023 versus 2021–2023), and non-identical spatial coverage (the newly delimited Almaty Region versus the former Almaty Region). No parcel-level correspondence between the two estimates was tested.

The near balance between the aggregate increase in agricultural land and the decreases in reserve and industrial land is arithmetically consistent with the official land balance, but it does not establish the direction, location, or parcel-level nature of any legal transfer. The 212.8 thousand ha decrease was therefore interpreted only as a change in the aggregate reserve-land category.

Settlement land remained stable at approximately 722.6–723.0 thousand ha during 2019–2021. Its area decreased to 291.7 thousand ha in 2022 as a consequence of administrative redelimitation and remained unchanged in 2023. The reduction should therefore be attributed to the 2022 division rather than to a process occurring in 2023.

Overall, the official statistics show that the 2022 reform changed the territorial basis of land accounting, whereas the 2022–2023 period was characterized by changes in the aggregate recorded legal categories within the new regional configuration. This distinction is essential because the first process is boundary-induced, while the second concerns changes among legally recorded land categories.

3.2 Land-fund structure on both sides of the new administrative boundary

To determine whether the 2022 reform changed only the total regional area or also the functional composition of the land fund, the two successor regions were compared using the official land balance immediately following the administrative division. Table 4 presents both the absolute areas and proportional shares of the principal land categories in the Almaty and Zhetysu Regions.

Table 4. Post-division land-fund structure of the Almaty and Zhetysu Regions as of 1 November 2022 [32]

Land Category	Almaty Region, thousand ha	Almaty Region, %	Zhetysu Region, thousand ha	Zhetysu Region, %	Difference, Percentage Points[1]
Agricultural land	4310.7	41.02	4633.8	39.11	+1.91
Settlement land	291.7	2.78	431.3	3.64	-0.86
Industrial, transport, communications, and other non-agricultural land	151.0	1.44	102.0	0.86	+0.58
Specially protected natural areas	962.3	9.16	680.4	5.74	+3.42
Forest fund land	2253.0	21.44	1499.8	12.66	+8.78
Water fund land	187.5	1.78	4.6	0.04	+1.74
Reserve land	2352.8	22.39	4496.3	37.95	-15.56
Total	10509.0	100.00	11848.2	100.00	-

Note: Percentage shares were calculated by the authors. [1]Almaty Region share minus Zhetysu Region share.

Although agricultural land represented similar shares in the Almaty and Zhetysu Regions (41.02% and 39.11%, respectively), their remaining land-fund structures differed markedly. Reserve land was more prominent in Zhetysu (37.95% versus 22.39%), whereas forest, protected, and water-fund land had larger shares in Almaty. Forest and protected land together accounted for 30.60% of Almaty and 18.40% of Zhetysu, and Almaty retained 97.6% of the combined water-fund land.

The reform therefore created different planning constraints rather than merely dividing the former territory. The larger environmental share in Almaty supports strict exclusion criteria, while the high reserve-land share in Zhetysu cannot be treated as immediate cultivation potential without soil, legal, and field verification [38]. The proportional differences in the land-fund structure of the two successor regions are visualized in Figure 3.

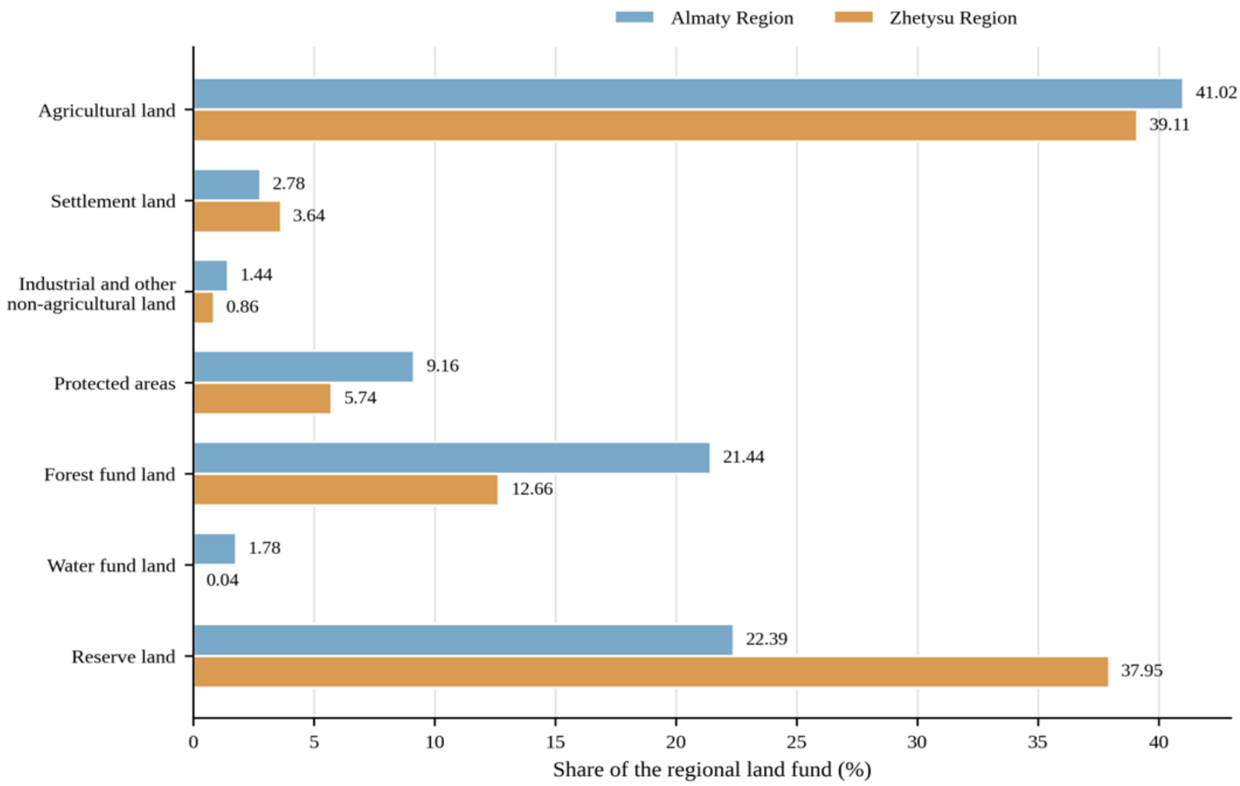

Figure 3. Comparison of the proportional land-fund structure of the Almaty and Zhetysu Regions immediately after the 2022 administrative division

3.3 Annual Normalized Difference Vegetation Index dynamics during 2019–2023

Annual growing-season NDVI composites provided a temporally consistent representation of vegetation conditions during the administrative-reform period. For direct inter-annual comparison, a common valid-observation mask covering approximately 8,443.0 thousand ha was used. Permanent water, snow and ice, pixels lacking comparable observations, and areas affected by persistent classification uncertainty were excluded from this mask.

The annual results showed inter-annual fluctuations, with lower mean and median NDVI values in 2023 than in 2019. The annual NDVI statistics and vegetation-density classes are presented in Table 5. A temporary increase was observed in 2021, followed by lower values in 2022 and 2023.

Table 5. Annual Normalized Difference Vegetation Index (NDVI) statistics and vegetation-density classes in the common analysis mask, 2019–2023

Year	Mean NDVI	Median NDVI	NDVI < 0.20, thousand ha	Share, %	NDVI 0.20–0.40, thousand ha	Share, %	NDVI > 0.40, thousand ha	Share, %
2019	0.218	0.184	6500	76.99	1720	20.37	223	2.64
2020	0.205	0.171	6770	80.18	1478	17.51	195	2.31
2021	0.211	0.178	6650	78.76	1580	18.71	213	2.52
2022	0.198	0.165	6810	80.66	1470	17.41	163	1.93
2023	0.191	0.157	6841	81.03	1444	17.10	158	1.87

Between 2019 and 2023, mean NDVI decreased from approximately 0.218 to 0.191, corresponding to a relative decline of 12.4%. Median NDVI decreased by approximately 14.7%, from 0.184 to 0.157. The larger proportional reduction in the median indicates that the decline was not restricted to a small number of extreme pixels but affected a substantial part of the common analysis area.

The area characterized by NDVI < 0.20 increased by approximately 341 thousand ha, or 5.25%, between 2019 and 2023. Its share of the common analysis mask increased from 76.99% to 81.03%. Conversely, the area with NDVI>0.40 decreased by approximately 65 thousand ha, or 29.1%. The moderately vegetated class also decreased, although less sharply, from approximately 1,720 to 1,444 thousand ha.

The 2021 composite interrupted the general downward sequence. Mean NDVI increased from 0.205 in 2020 to approximately 0.211 in 2021, and the area with NDVI > 0.40 increased from approximately 195 to 213 thousand ha. Because the series contained only five annual observations, this short-lived increase was interpreted as inter-annual variability rather than evidence of a sustained long-term trend.

The trajectory classification indicated that approximately 70.8% of the common analysis area remained within the stable range of $|\beta| < 0.01$ NDVI units per year, 18.6% showed decreasing NDVI values, and 10.6% showed increasing values. Decreasing NDVI values were observed in parts of the Ili, Karasai, Talgar, and Enbekshikazakh districts, whereas increasing values occurred more locally. Because precipitation and other climatic or land-management variables were not analyzed, these spatial patterns cannot be attributed to either land-use change or climate variability.

The reduction in high-NDVI territory and increase in low-NDVI territory are consistent with the authors' previous analysis of the Almaty Region [22], which compared 2015, 2020, and 2023. That earlier study also reported a reduction in areas with high NDVI and an increase in areas with low values, but it did not describe annual trajectories during the administrative-reform period.

It is important that NDVI < 0.20 is not interpreted automatically as land degradation. Low values may represent bare ground, fallow fields, recently harvested cropland, built-up areas, sparse natural vegetation, or genuinely degraded land. The annual NDVI analysis therefore characterizes vegetation density, while the physical nature of the changes is evaluated separately through the land-cover transition matrix. The annual vegetation dynamics and spatial distribution of NDVI trajectory classes are presented in Figure 4.

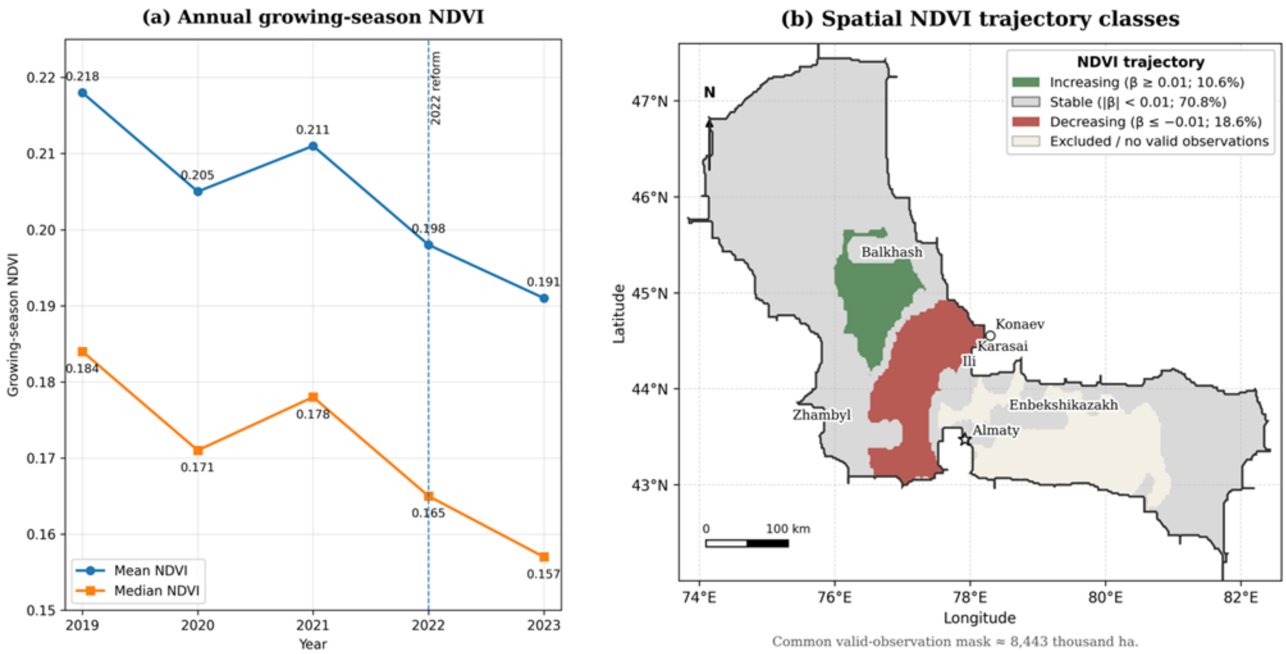

Figure 4. Annual vegetation dynamics during 2019–2023: (a) mean and median growing-season NDVI; and (b) spatial distribution of pixel-wise NDVI trajectory classes

Note: The Normalized Difference Vegetation Index (NDVI) classes used in the annual summaries were NDVI < 0.20, 0.20 ≤ NDVI ≤ 0.40, and NDVI > 0.40. Trajectories were classified as increasing when $\beta \geq 0.01$ NDVI units year^{-1}, stable when $|\beta| < 0.01$, and decreasing when $\beta \leq -0.01$. Excluded cells lacked sufficient valid annual observations.

Source: Prepared by the authors using Sentinel-2 Level-2A data [32, 33].

Table 6. Land-cover transition matrix for the former Almaty Region between 2021 and 2023, thousand ha

2021 Class / 2023 Class	Cropland	Grass and Shrub Cover	Tree Cover	Built-Up Land	Bare Ground	Water and Wetland	Total 2021
Cropland	1640	120	5	35	45	5	1850
Grass and shrub cover	260	13480	60	30	160	10	14000
Tree cover	5	45	2410	5	20	15	2500
Built-up land	2	3	0	242	3	0	250
Bare ground	80	210	5	18	2467	20	2800
Water and wetland	0	42	0	0	85	473	600
Total 2023	1987	13900	2480	330	2780	523	22000

3.4 Land-cover transitions between 2021 and 2023

The land-cover change analysis was conducted independently of the official legal land-category comparison. Tables 3 and 4 describe changes in legally defined land categories before and after the administrative reorganization, whereas Table 6 represents physical land-cover classes recorded for the same grid cells within the common analysis mask in 2021 and 2023.

The valid land-cover comparison covered approximately 22,000.0 thousand ha of the former Almaty Region. Approximately 357.2 thousand ha were excluded because of snow, cloud, missing data, or other classification uncertainty. Together, the valid and excluded areas sum to 22,357.2

thousand ha, matching the official total area of the former Almaty Region.

Stable classes on the main diagonal accounted for approximately 20712 thousand ha, or 94.15% of the valid comparison area. The remaining 1288 thousand ha, or 5.85%, displayed a change between the two annual classifications. The high stable share is expected in a two-year regional comparison and confirms that the principal spatial structure of the former region remained unchanged.

The largest expansion-related transition was from grass and shrub cover to cropland, covering approximately 260 thousand ha. An additional 80 thousand ha changed from bare ground to cropland. These two transitions together represented approximately 340 thousand ha of newly detected cropland.

Changes in the opposite direction were also observed. Approximately 120 thousand ha of cropland changed to grass and shrub cover, while approximately 45 thousand ha changed to bare ground. A further 35 thousand ha of cropland changed to built-up land. The resulting net increase in the satellite-derived cropland class was approximately 137 thousand ha.

The approximately 137 thousand ha net change in the satellite-derived cropland class is reported exclusively as a physical land-cover result. It is not a spatial or numerical estimate of the official 216.0 thousand ha increase in agricultural land. The official agricultural-land category may include pasture, hayfield, fallow land, perennial plantations, farm infrastructure, and other non-cropland surfaces, whereas the satellite cropland class represents the dominant physical surface signal. In addition, the temporal and spatial extents of the two analyses are not identical.

The spatial comparison indicated that approximately 151 thousand ha of the grass/shrub-to-cropland transition and 45 thousand ha of the bare-ground-to-cropland transition occurred within the present Almaty Region. The corresponding estimates for the Zhetysu Region were approximately 109 and 35 thousand ha, respectively.

Cropland expansion in the present Almaty Region was concentrated mainly in the agricultural belts of the Enbekshikazakh, Zhambyl, Ili, and western Balkhash districts. In the Zhetysu Region, comparable transitions were distributed across the agricultural territories of the Karatal, Koksu, Panfilov, and Alakol districts.

Approximately 29 thousand ha of the detected cropland-to-built-up transition occurred within the present Almaty Region, compared with approximately 6 thousand ha in the Zhetysu Region. The higher concentration in the Almaty Region is spatially consistent with peri-urban development around the Almaty metropolitan area, particularly in the Ili, Karasai, and Talgar districts.

Cropland-to-grass/shrub transitions were more evenly distributed: approximately 58 thousand ha occurred in the present Almaty Region and approximately 62 thousand ha in the Zhetysu Region. These areas may include temporary fallow land, crop rotation, abandoned fields, classification variability, or actual withdrawal from cultivation. They should not be interpreted as permanent agricultural decline without multi-year confirmation.

Figure 5 therefore provides the spatial information missing from the initial area-only analysis. It identifies both the direction of the principal physical transitions and the areas in which they were concentrated. At the same time, none of these satellite-derived transitions proves a legal cadastral transfer from reserve land to agricultural land.

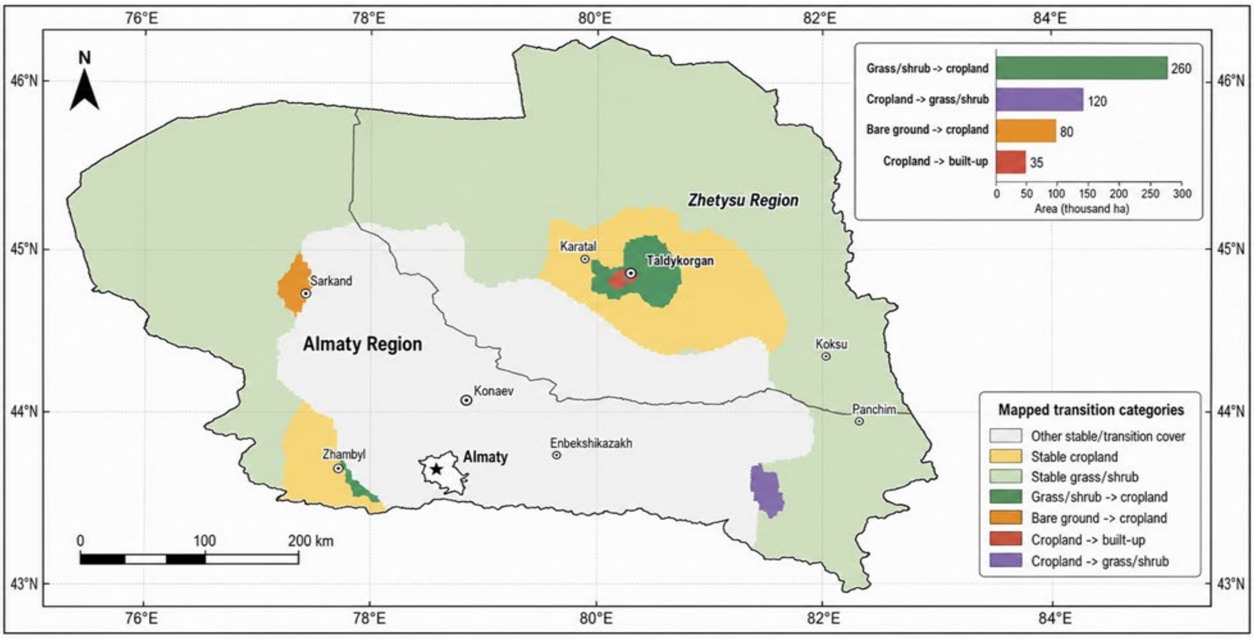

Figure 5. Major physical land-cover transitions between 2021 and 2023 within the former Almaty Region

Note: The mapped categories include stable cropland, stable grass and shrub cover, grass/shrub-to-cropland, bare-ground-to-cropland, cropland-to-built-up land, and cropland-to-grass/shrub transitions; the remaining stable and transition classes are grouped as other stable/transition cover.

Source: Prepared by the authors through post-classification comparison of the 2021 and 2023 Esri/Impact Observatory 10-m land-use/land-cover maps [21]. Administrative boundaries were obtained from SimpleMaps [31] and verified against Presidential Decree No. 887 [14].

3.5 Contextual district-level agricultural specialization

A district-level crop dataset was used to interpret the spatial distribution of the modeled priority areas. Because the dataset includes the city of Alatau, which was established in 2024, it was treated as a contextual post-study snapshot rather than as part of the 2019–2023 temporal series. The complete district-level values are presented in Table A1.

The dataset indicates a pronounced territorial concentration of agricultural production. The Zhambyl and Enbekshikazakh districts jointly accounted for approximately 52.8% of the reported cereal area. The Enbekshikazakh, Zhambyl, and Ili districts accounted for 80.3% of the oilseed area.

Vegetable production was concentrated primarily in the Enbekshikazakh and Karasai districts, which together represented approximately 65.3% of the reported open-ground vegetable area. The Karasai, Raiymbek, and Zhambyl districts accounted for 74.1% of potato area, while the Enbekshikazakh and Ili districts represented approximately 59.3% of forage-maize area.

These concentrations describe agricultural specialization but do not independently establish its causes. Nevertheless, the spatial pattern is consistent with the combined influence of irrigation availability, established production systems, terrain, road access, and proximity to the Almaty consumer market.

The specialization data were used only to support interpretation of the scenario outputs. They were not included in the calculation of the 2019–2023 land-fund trends, annual NDVI trajectories, or 2021–2023 land-cover transitions.

3.6 Multi-criteria suitability and scenario results

After applying the hard spatial constraints, approximately 4,920.0 thousand ha, or 46.8% of the newly delimited Almaty Region, remained eligible for comparative suitability assessment. The excluded area included forest and tree-covered land, built-up territory, water and wetlands, specially protected natural areas, slopes exceeding 15°, protective buffers around permanent water bodies, and cells lacking reliable input data.

The three scenarios produced different distributions of high-suitability and selected priority land. Their results are summarized in Table 7.

Table 7. Results of the balanced, conservation-oriented, and production-accessibility scenarios

Indicator	Balanced Scenario	Conservation-Oriented Scenario	Production-Accessibility Scenario
Eligible area, thousand ha	4920.0	4920.00	4920.0
Low suitability, thousand ha	875.0	1060.0	720.0
Moderately low suitability, thousand ha	1288.0	1062.0	1455.0
Moderate suitability, thousand ha	2145.0	2360.0	2010.0
High suitability, thousand ha	612.0	438.0	735.0
High suitability, % of eligible area	12.44	8.90	14.94
Priority area after the 10% quota and cluster filtering, thousand ha	476.4	461.2	483.0
Priority area, % of total regional area	4.53	4.39	4.60
Number of priority clusters	83	71	96
Mean cluster area, thousand ha	5.74	6.50	5.03
Jaccard coefficient under ±10% weight variation	0.82	0.86	0.74
Unconstrained candidate cells removed by the exclusion mask, %	16.3	15.2	17.1

3.6.1 Balanced scenario

The balanced scenario identified approximately 612.0 thousand ha as highly suitable, representing 12.44% of eligible land. After application of the top-10% quota and removal of isolated clusters smaller than 25 ha, approximately 476.4 thousand ha remained in 83 spatially coherent priority clusters.

The principal balanced-scenario clusters were located in the Enbekshikazakh, Zhambyl, Ili, and western Balkhash districts. These zones combined moderate or high growing-season NDVI, slopes generally below 8°, and comparatively favourable access to roads, settlements, and mapped water or irrigation features.

The balanced scenario produced a Jaccard stability coefficient of approximately 0.82 under the ±10% weight-variation test. This indicates that most high-priority cells remained selected after moderate changes in criterion weights.

3.6.2 Conservation-oriented scenario

The conservation-oriented scenario produced the smallest high-suitability area, approximately 438.0 thousand ha, or 8.90% of eligible territory. After cluster filtering, approximately 461.2 thousand ha remained within the scenario-specific top-decile priority set.

The apparent difference between the high-suitability class and the final priority area occurred because the priority selection involved two sequential steps. First, cells were ranked by suitability score and selected from both the high and upper-moderate suitability classes until the common 10% area quota was reached. Second, isolated clusters smaller than 25 ha were removed to obtain spatially coherent priority areas.

Priority zones were more spatially compact and shifted away from steep foothill areas, tree-covered zones, and environmentally sensitive territory. Larger clusters occurred in the lower-slope parts of the Balkhash, Zhambyl, and northern Enbekshikazakh districts. The conservation scenario generated 71 clusters with the largest mean cluster area, approximately 6.50 thousand ha.

Its Jaccard coefficient of approximately 0.86 was the highest among the scenarios, indicating comparatively strong spatial stability. This result reflects the greater influence of slope and current land cover, which limited the number of alternative eligible locations.

3.6.3 Production-accessibility scenario

The production-accessibility scenario identified approximately 735.0 thousand ha as highly suitable, or 14.94% of eligible land. Following the common quota and cluster filtering, approximately 483.0 thousand ha remained in 96 priority clusters.

Priority areas were concentrated along accessible agricultural and peri-urban corridors, particularly in the Ili, Enbekshikazakh, Zhambyl, Karasai, and Talgar districts. The increased weights assigned to NDVI, water accessibility, and road proximity expanded the high-suitability class but also produced a more fragmented spatial pattern.

The production-accessibility scenario had a Jaccard coefficient of approximately 0.74, indicating moderate sensitivity to criterion-weight changes. Its lower stability reflects competition among road access, market proximity, vegetation condition, and water accessibility in intensively used peri-urban territory.

3.6.4 Comparison of the scenarios

Approximately 312.6 thousand ha were included in the priority set under all three scenarios. This common area represented 65.6% of the balanced priority area, 67.8% of the conservation-oriented priority area, and 64.7% of the production-accessibility priority area. These consistently selected zones constitute the most robust regional priorities for subsequent cadastral, soil, water, and field assessment.

Applying the hard exclusion mask removed approximately 15.2–17.1% of cells that would otherwise have entered the top-decile candidate set in an unconstrained weighted-overlay model. This result should be interpreted as avoidance of potential planning conflicts, not as a measured 15–17% reduction in existing legal disputes or land-use conflicts.

The official land balance records 2.14 million ha of reserve land in the Almaty Region in 2023, whereas the model identified 438.0–735.0 thousand ha as highly suitable and 461.2–483.0 thousand ha as final priority land, depending on the scenario. These quantities are not directly comparable because reserve land is an aggregate legal category and the modeled areas are raster-based physical and accessibility classes. Their spatial overlap is unknown because a complete georeferenced reserve-land layer was unavailable. Consequently, the modeled areas cannot be described as a suitable subset of reserve land.

The scenario results instead identify areas whose physical and accessibility characteristics justify subsequent examination. Legal status, soil quality, erosion risk, irrigation feasibility, water rights, and actual land use must be verified before any planning or cadastral decision is made. The spatial distribution of suitability scores and priority areas under the three scenarios is presented in Figure 6.

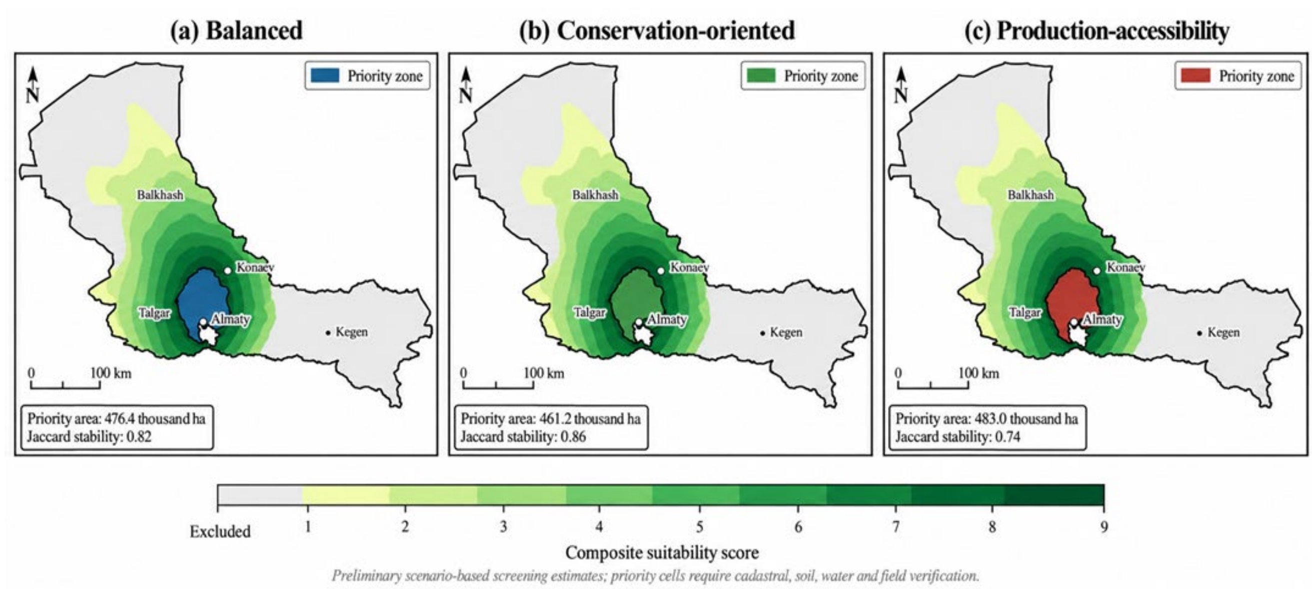

Figure 6. Composite agricultural-suitability scores and final priority areas under the (a) balanced, (b) conservation-oriented, and (c) production-accessibility scenarios

Note: Suitability classes were defined as low ($S_i < 3.0$), moderately low ($3.0 \leq S_i < 5.0$), moderate ($5.0 \leq S_i < 7.0$), and high ($S_i \geq 7.0$). Excluded areas are shown in light grey and comprise water and wetlands, tree-covered and built-up areas, specially protected natural areas, slopes exceeding 15°, the 100-m buffer around permanent water bodies, and cells lacking reliable input data. The colored overlays indicate the scenario-specific priority zones selected after application of the 10% area quota and removal of clusters smaller than 25 ha.

Source: Prepared by the authors using the datasets and procedures described in Sections 2.7–2.9.

3.7 Integrated discussion and methodological implications

The combined results demonstrate that administrative change, legal land-category redistribution, vegetation dynamics, physical land-cover conversion, and modeled agricultural suitability are related but methodologically distinct processes.

First, the 53% reduction in the reported area of the Almaty Region between 2021 and 2022 did not represent physical land loss. It resulted from the establishment of the Zhetysu Region. Comparisons that ignore this boundary change would incorrectly interpret an administrative event as a dramatic land-use transformation.

Second, the division created two regions with different structural constraints. The Zhetysu Region received a substantially larger proportion of reserve land, whereas the Almaty Region retained higher shares of forest, protected, and water fund land. Consequently, the newly delimited Almaty Region has a smaller proportion of territory that can reasonably be considered for agricultural expansion without first applying environmental and functional exclusions.

The official 2022–2023 land balance recorded a decrease of 212.8 thousand ha in reserve land and an increase of 216.0 thousand ha in agricultural land. These values describe changes in aggregate legal-category totals. The separate satellite analysis identified physical transitions among cropland, grass and shrub cover, bare ground, built-up land, tree cover, and water-related classes. Because legal parcel boundaries were unavailable and the analyses differed in period and spatial coverage, the official and satellite estimates cannot be matched or interpreted as measurements of the same conversion process.

The transition matrix suggests that grass and shrub cover was the main source of newly detected cropland, accounting for approximately 260 thousand ha, followed by bare ground at approximately 80 thousand ha. At the same time, approximately 200 thousand ha of cropland changed to grass/shrub, bare ground, built-up land, tree cover, or water-related classes. This bidirectional pattern shows that regional agricultural change cannot be represented as a single one-way conversion from reserve to active land.

The annual NDVI series showed inter-annual variability and lower mean and median values in 2023 than in 2019. However, precipitation and other climatic or land-management variables were not included in the analysis; consequently, the observed NDVI changes cannot be attributed to land-use change or climate variability. The five-year slopes should therefore be interpreted only as descriptive indicators of vegetation conditions during the study period.

The spatial model also shows that suitability depends strongly on the planning objective. Increasing the importance of production and accessibility expanded the high-suitability class but reduced stability and increased spatial fragmentation. Giving greater weight to slope and current land cover reduced the highly suitable area but produced more stable and compact clusters. However, the weighting scheme reflects author-defined study assumptions rather than formal expert or stakeholder validation. Consequently, the ranking of priority areas is conditional on these assumptions and requires external validation before operational planning.

The scenario comparison demonstrates that the phrase "optimal agricultural land" should be used cautiously. A spatial cell may obtain a high suitability score because of favourable vegetation, slope, and accessibility, while remaining legally unavailable, lacking reliable irrigation, being affected by erosion, or requiring soil rehabilitation. Model outputs should therefore support prioritization of field investigations rather than replace cadastral and environmental decision-making.

Several limitations affect the interpretation of the results. The Esri/Impact Observatory product has an assessed average global accuracy exceeding 75%, but class-specific uncertainty remains higher for rangeland and bare ground than for water, tree cover, built-up land, and cropland. OpenStreetMap coverage may vary among districts, particularly for minor irrigation canals and rural roads. These omissions limit the use of the results for parcel-level precision agriculture.

Finally, the numerical outputs of the NDVI, transition, and suitability analyses should be treated as regional screening estimates. Their principal contribution is to provide a coherent analytical framework in which official land statistics and satellite-derived land-cover changes are analyzed separately and interpreted as complementary but non-equivalent evidence, with explicitly defined objectives, decision variables, constraints, scenario rules, and sensitivity procedures.

4. CONCLUSIONS

This study separately analyzed changes in official land accounts, satellite-derived land cover, vegetation conditions, and scenario-based agricultural suitability and interpreted these results as complementary but non-equivalent evidence. The 53.0% decrease in the reported area of the Almaty Region between 2021 and 2022 resulted from the creation of the Zhetysu Region rather than physical land loss. Within the newly delimited region, official agricultural land increased by 216.0 thousand ha and reserve land decreased by 212.8 thousand ha between 2022 and 2023; however, these aggregate legal-category changes were not matched to individual parcels. The separate 2021–2023 satellite analysis identified bidirectional physical land-cover transitions and an approximately 137 thousand ha net cropland gain over the former regional territory. This value is not directly comparable with the official change because the objects, classification systems, periods, and spatial coverage differ. Mean and median growing-season NDVI were lower in 2023 than in 2019, but the observed variation cannot be attributed to climatic or human drivers without concurrent precipitation and management data. Across the three suitability scenarios, approximately 312.6 thousand ha formed a common priority core. Its overlap with legally designated reserve land remains unknown; therefore, the identified zones should be treated as priorities for subsequent cadastral, soil, water, and field verification rather than as land recommended directly for agricultural conversion.

REFERENCES

[1] Zhilyakov, D., Petrushina, O., Meshcheryakov, K., et al. (2025). Enhancing food security in Central Asia and the Caucasus: A SWOT analysis of agro-industrial potential. International Journal of Safety and Security Engineering, 15(7): 1461-1470. https://doi.org/10.18280/ijsse.150713

[2] Tleshpayeva, D., Bondarenko, N., Leontev, M., et al. (2025). Assessment of economic management of land resources to enhance food security. Qubahan Academic Journal, 5(1): 159-168. https://doi.org/10.48161/qaj.v5n1a1048

[3] Semenikhina, S., Keubassova, G., Kalieva, A., et al. (2025). Needle-based assessment of urban and industrial air pollution in Aktobe. World Journal of Environmental Biosciences, 14(3): 110-119. https://doi.org/10.51847/il1jiJHVsy

[4] Yskak, A., Tsvetnov, E.V., Marakhova, N.A., Nugmanov, A., Irzhanov, Z.B. (2026). Proficiency in the conceptualization and assessment of land degradation: A review. SABRAO Journal of Breeding and Genetics, 58(2): 922-932. http://doi.org/10.54910/sabrao2026.58.2.42

[5] Yesmagulova, B., Jigildiyeva, Z., Tassanova, Z., et al. (2026). Remote sensing and GIS-based monitoring of land degradation in the Bokey Orda District, West Kazakhstan. International Journal of Agriculture and Biosciences 15(1): 159-167. https://doi.org/10.47278/journal.ijab/2025.159

[6] Malamataris, D., Ganoulis, P., Galiatsatou, P., et al. (2026). How do changes in land use and land cover aggravate the flooding hazard? GeoHazards, 7(3): 82. https://doi.org/10.3390/geohazards7030082

[7] Yao, J., Zhang, X.X., Murray, A.T. (2017). Spatial optimization for land-use allocation: Accounting for sustainability concerns. International Regional Science Review, 41(6): 579-600. https://doi.org/10.1177/0160017617728551

[8] Ziadat, F., Bunning, S., De Pauw, E. (2017). Land resources planning for sustainable land management. Food and Agriculture Organization of the United Nations, Rome. https://openknowledge.fao.org/handle/20.500.14283/i5937en.

[9] Ussipbayev, G., Omarbekova, A., Aidarova, A.,

Ussipbayev, N., Sagandykova, D. (2025). Sustainable land use formation features on agricultural land in Kazakhstan. RIVAR, 12(34): 208-222. https://doi.org/10.35588/7ds80736
[10] Kyrgyzbay, K., Kakimzhanov, Y., Sagin, J. (2023). Climate data verification for assessing climate change in Almaty region of the Republic of Kazakhstan. Climate Services, 32: 100423. https://doi.org/10.1016/j.cliser.2023.100423
[11] Savin, T., Morgounov, A. (2025). Organic crop production in Kazakhstan: Agronomic solutions and bioresources. Resources, 14(7): 108. https://doi.org/10.3390/resources14070108
[12] Sarsekova, D., Sagin, J., Perzadayeva, A., et al. (2026). Farmers' land sustainability improvement with soil, geology, and water retention assessment in North Kazakhstan. Sustainability, 18(3): 1316. https://doi.org/10.3390/su18031316
[13] Aidarova, A., Omarbekova, A., Ussipbayev, G., Onalbayeva, D., Mauyayeva, S. (2024). Improvement of methods of rational use in conditions of land degradation in the Almaty Region, Karasai District. Scientific Horizons, 27(9): 110-120. https://doi.org/10.48077/scihor9.2024.110
[14] Smailov, A. (2022). Resolution of the Government of the Republic of Kazakhstan. On certain issues regarding the implementation of the decrees of the President of the Republic of Kazakhstan dated May 3, 2022 No. 886 "On certain issues of the administrative-territorial structure of the Republic of Kazakhstan" and dated May 3, 2022 No. 887 "On certain issues of the administrative-territorial structure of the Republic of Kazakhstan". https://prg.kz/document/?doc_id=33223597.
[15] Klein, I., Garcia Boadas, E., van der Voort, C.R., et al. (2026). An integrated earth observation assessment of land-cover change, settlement expansion, and tropospheric NO_2 in East Kazakhstan. Land, 15(8): 1513. https://doi.org/10.3390/land15081513
[16] Mohamed, M.A., Anders, J., Schneider, C. (2020). Monitoring of changes in land use/land cover in Syria from 2010 to 2018 using multitemporal Landsat imagery and GIS. Land, 9(7): 226. https://doi.org/10.3390/land9070226
[17] Prado, P.E., Oporto, C.G., Jönsson, K., Rejas, D., Martinez, V., Persson, K.M. (2025). Influence of land use/land cover on stream water quality in two watersheds in the central Andes of Bolivia: An optimised methodology. Ecological Indicators, 178: 113984. https://doi.org/10.1016/j.ecolind.2025.113984
[18] Rafikov, T., Zhumatayeva, Z., Mukaliyev, Z., Zhildikbayeva, A. (2024). Evaluating land degradation in East Kazakhstan using NDVI and Landsat data. International Journal of Design & Nature and Ecodynamics, 19(5): 1677-1686. https://doi.org/10.18280/ijdne.190521
[19] Shokparova, D.K., Sirazhitdinova, M., Bissenbayeva, S.B., Patel, N. (2025). Remote sensing and GIS-based land assessment in Zhanaarka region of Ulytau oblast, Kazakhstan. Frontiers in Environmental Science, 13: 1516460. https://doi.org/10.3389/fenvs.2025.1516460
[20] Alipbeki, O., Alipbekova, C., Mussaif, G., et al. (2024). Analysis and prediction of land use/land cover changes in Korgalzhyn District, Kazakhstan. Agronomy, 14(2): 268. https://doi.org/10.3390/agronomy14020268
[21] Karra, K., Kontgis, C., Statman-Weil, Z., Mazzariello, J.C., Mathis, M., Brumby, S.P. (2021). Global land use / land cover with Sentinel-2 and deep learning. In 2021 IEEE International Geoscience and Remote Sensing Symposium IGARSS, Brussels, Belgium, pp. 4704-4707. https://doi.org/10.1109/IGARSS47720.2021.9553499
[22] Zhusupov, E., Zhildikbayeva, A., Rafikov, T., Kanatbek, A. (2025). Analysis of vegetation cover dynamics in the Almaty Region based on NDVI and geoinformation technologies. Izdenister Natigeler, 3(107): 518-526. https://doi.org/10.37884/3-2025/50
[23] Onalbayeva, D., Omarbekova, A., Zhumasylova, A., Cherniyazova, U., Gurskiene, V. (2026). Geoinformation analysis of agricultural land use: A case study of the Almaty Region. Izdenister Natigeler, 28(1(109)): 155-168. https://doi.org/10.37884/1-2026/16
[24] Yao, J., Murray, A.T., Wang, J., Zhang, X.X. (2019). Evaluation and development of sustainable urban land use plans through spatial optimization. Transactions in GIS, 23(4): 705-725. https://doi.org/10.1111/tgis.12531
[25] Hasti, F., Salmanmahiny, A., Rouhi, H., Sakieh, Y., Joolaei, R., Pezhooli, N. (2023). Developing an integrated land allocation model based on linear programming and game theory. Environmental Monitoring and Assessment, 195: 493. https://doi.org/10.1007/s10661-023-11124-w
[26] Rahman, M. M., Szabó, G. (2021). Multi-objective urban land use optimization using spatial data: A systematic review. Sustainable Cities and Society, 74: 103214. https://doi.org/10.1016/j.scs.2021.103214
[27] Cao, K. (2017). Spatial optimization for sustainable land use planning. In Comprehensive Geographic Information Systems, pp. 244-252, Elsevier. https://doi.org/10.1016/b978-0-12-409548-9.09603-2
[28] Altunina, Y., Korotun, O., Polevshchikov, I. (2024). Simulation model of a queuing system in the service of state registration, cadastre and cartography. E3S Web of Conferences, 535: 05003. https://doi.org/10.1051/e3sconf/202453505003
[29] Xiao, J.Y., Dai, J.J., Chen, L.Q., Song, Y. (2024). The identification of land use conflicts and policy implications for Donghai County based on the "Production–Living–Ecological" functions. Land, 13(12): 2013. https://doi.org/10.3390/land13122013
[30] Han, H., Zhang, K., Ma, G. (2025). Changes in land use conflict and zoning optimization in rapidly developing mountainous cities: A case study of Guiyang, China. Journal of Environmental Engineering and Landscape Management, 33(3): 284-298. https://doi.org/10.3846/jeelm.2025.24555
[31] SimpleMaps. (2026). Free Kazakhstan GIS map files. https://simplemaps.com/gis/country/kz.
[32] Committee or Land Administration of the Ministry of Agriculture of the Republic of Kazakhstan. https://www.gov.kz/memleket/entities/land/documents/1?lang=en.
[33] European Space Agency. (2015). Sentinel-2 User Handbook. European Commission. https://sentinels.copernicus.eu/documents/247904/685211/Sentinel-2_User_Handbook.
[34] Google Earth Engine Data Catalog. (2026). Harmonized Sentinel-2 MSI: MultiSpectral Instrument, Level-2A Surface Reflectance. European Union/ESA/Copernicus.

https://developers.google.com/earth-engine/datasets/catalog/COPERNICUS_S2_SR_HARMONIZED?hl=zh-cn.
[35] European Space Agency, European Union, and Airbus. (2023). Copernicus DEM - Global and European Digital Elevation Model. https://doi.org/10.5270/ESA-c5d3d65
[36] OpenStreetMap contributors. (2024). OpenStreetMap Data for Kazakhstan: Extract Dated 1 January 2024. Geofabrik GmbH. Open Database License 1.0. https://download.geofabrik.de/asia/kazakhstan.html.
[37] Sustainable forest management toolbox. Forest and water. Food and Agriculture Organization of the United Nations, Rome. https://www.fao.org/sustainable-forest-management/toolbox/modules/forest-and-water/tools/en/.
[38] Abaikyzy, M., Yerkinbayeva, L.K., Aidarkhanova, K.N., Aigarinova, G.T., Baimbetov, N.S. (2020). The formation of land conservation principles as the framework for the implementation of the concept of sustainable development of society. Journal of Landscape Ecology, 13(3): 23-38. https://doi.org/10.2478/jlecol-2020-0015

APPENDIX

Table A1. Contextual district-level distribution of selected crop areas in the Almaty Region in 2024, ha

Administrative Unit	Cereals	Winter and Spring Wheat	Oilseeds	Sunflower	Open-Ground Vegetables	Melons and Gourds	Potatoes	Forage Maize
Almaty Region	170,158.3	42,663.5	24,528.1	1,984.2	15,512.5	1,849.4	10,418.7	9,731.0
City of Konaev	3,049.5	255.0	523.0	–	577.5	289.2	93.6	1,482.0
City of Alatau	2,065.0	683.0	2,110.0	–	999.6	–	99.9	270.0
Balkhash District	12,941.7	5,066.8	–	–	118.9	56.5	119.1	150.0
Enbekshikazakh District	39,633.3	2,569.9	9,986.7	155.2	7,315.9	32.7	616.2	3,236.5
Zhambyl District	50,225.5	12,450.0	5,044.0	1,720.0	1,141.3	695.0	1,621.0	890.0
Kegen District	7,308.0	3,302.0	–	–	134.0	–	691.8	–
Karasai District	10,728.6	1,535.8	386.4	–	2,815.4	69.0	3,866.3	50.0
Raiymbek District	12,212.4	7,992.5	–	–	10.0	–	2,233.0	–
Talgar District	10,294.5	2,743.0	1,807.0	88.0	715.0	87.5	688.2	1,070.0
Uygur District	5,831.8	821.5	20.0	20.0	431.5	77.5	86.8	50.0
Ili District	15,868.0	5,244.0	4,651.0	1.0	1,253.4	542.0	302.8	2,532.5